

Clear Signatures of Specific Inelastic and Transfer Channels in the Distribution of Fusion Barriers

C. R. Morton, M. Dasgupta, D. J. Hinde, J. R. Leigh, R. C. Lemmon, J. P. Lestone,
J. C. Mein, J. O. Newton, and H. Timmers

*Department of Nuclear Physics, Research School of Physical Sciences and Engineering,
Australian National University, Canberra, Australian Capital Territory 0200, Australia*

N. Rowley*

*Department of Physics, University of Manchester, Manchester M13 9PL, United Kingdom
and Department of Physics, University of Surrey, Guildford GU2 5XH, United Kingdom*

A. T. Kruppa

*Institute of Nuclear Research of the Hungarian Academy of Sciences, Debrecen, Pf 51, Hungary
(Received 2 February 1994)*

Fusion excitation functions for $^{144}\text{Sm} + ^{16}\text{O}$ and ^{17}O have been measured to high precision. The extracted fusion barrier distributions show a double-peaked structure which is interpreted in terms of coupling to inelastic excitations of the target. The effect of the neutron stripping channel is evident in the reaction with ^{17}O . These barrier distributions show clearly the signatures of specific inelastic and transfer channels.

PACS numbers: 25.70.Jj

The complex interactions between composite particles are often approximated by an effective central potential. The influence of internal degrees of freedom on this potential is a general problem in many branches of physics and chemistry, and is of fundamental importance in describing the phenomena which may occur during a collision. In the case of the fusion of heavy nuclei, the coupling between the relative motion and internal degrees of freedom causes a splitting in energy of the uncoupled fusion barrier. The resultant distribution of fusion barriers has a shape indicative of the relevant couplings, and is directly manifested as an enhancement of the fusion cross section at energies below the uncoupled barrier. The latter is well known, and, in many previous investigations, cross-section data have been fitted by the successive inclusion of channels *expected* to be important [1-7]. This approach was at the time reasonable, since the value of very precise cross-section measurements was not realized.

Recently, it has been shown that fusion excitation functions can be simply transformed to reveal directly the distribution of barriers as a function of energy [8]. The barrier distribution from precision measurements of fusion cross sections for the $^{154}\text{Sm}+^{16}\text{O}$ reaction showed the very distinctive shape due to strong coupling to the ground-state rotational band ($0^+ \rightarrow 2^+, 4^+, \dots$) of ^{154}Sm . Moreover, the extracted quadrupole and hexadecapole deformation parameters agreed with those from nonfusion studies [9,10]. The barrier distribution is also sensitive to relatively weaker couplings [11], however, in the presence of strong coupling effects, the small perturbations caused by the former make it difficult to identify them unambiguously. By choosing ^{144}Sm as a target, which has no low-lying rotational states, such strong cou-

pling effects should be absent, and hence allow investigation of the influence of more weakly coupled individual channels.

This Letter demonstrates that precisely determined fusion excitation functions can give quantitative information about the weakly coupled inelastic and transfer channels influencing the fusion process, including their coupling strengths.

The experiments were performed with the 14UD tandem accelerator at the Australian National University. Targets of ^{144}Sm , isotopically enriched to 96.5%, with areal densities of $\simeq 40 \mu\text{g cm}^{-2}$ were bombarded with pulsed $^{16,17}\text{O}$ beams in an energy range of $61 \leq E_{\text{lab}} \leq 100$ MeV. Excitation functions for evaporation residues (ER) were measured at $\pm 2^\circ$ to the beam axis using a compact velocity filter [12] to deflect the intense elastically scattered beam. The residues were detected in a multiwire proportional counter positioned behind the filter and were identified by their time of flight with respect to the pulsed beam and their energy loss in the detector. A beam energy calibration performed in conjunction with these measurements, using the 14.23 MeV resonance in the $^{12}\text{C}(p, \alpha)^9\text{Be}$ reaction, defined the projectile energy to better than ± 0.05 MeV [13]. Total ER cross sections were obtained by normalization of the measured differential cross sections at $\pm 2^\circ$ with measurements of full angular distributions as described in Ref. [9]. The total fusion cross section is equal to the ER cross section since fission for this system is negligible. The uncertainties in the cross sections were less than 1 mb for energies up to $E_{\text{c.m.}} = 63$ MeV, and were $\pm 1\%$ for the higher energies. All six heavier samarium isotopes were present at $\lesssim 1\%$ levels in the target. Corrections to the measured cross

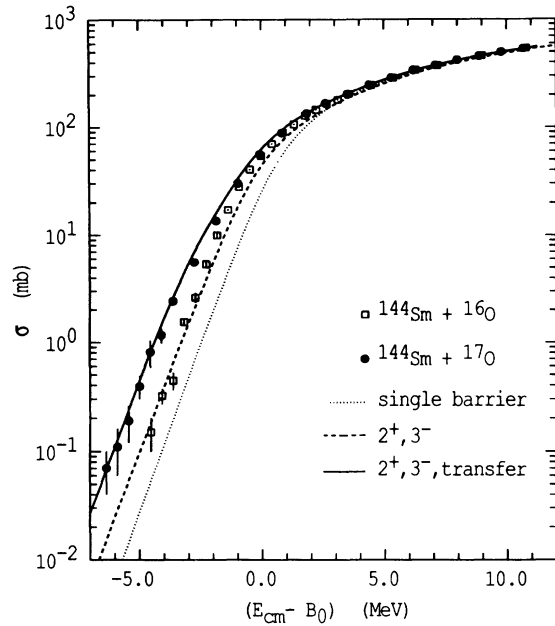


FIG. 1. The experimental fusion excitation functions for the $^{144}\text{Sm}+^{16,17}\text{O}$ reactions as a function of the difference between the center of mass energy and the respective average barriers. In the low energy region, the ^{17}O cross sections are up to 4 times greater than those for the ^{16}O reaction. The dotted line is the cross section for a single barrier obtained by fitting to the high energy data. The dashed and solid lines are theoretical calculations for the ^{16}O and ^{17}O reactions, respectively (see text).

sections were made using calculations which systematically reproduced the experimental results presented in Refs. [9,14].

The measured fusion cross sections $\sigma(E)$ for the $^{144}\text{Sm}+^{16,17}\text{O}$ reactions are shown in Fig. 1 as a function of the difference between the center of mass energy and the average barrier ($E_{c.m.} - B_0$) for each system. Only at energies below B_0 do the data differ significantly, the ^{17}O induced reaction giving cross sections up to 4 times larger. This difference will be discussed later.

The first step in the analysis of these data was to fit the high energy cross sections, where $E_{c.m.} - B_0 \geq 4$ MeV, using a single barrier. The diffuseness a and depth of a Woods-Saxon nuclear potential were varied, the best fit occurring for $a = 0.80 \pm 0.10$ fm, corresponding to an s -wave barrier height $B_0 = 61.11$ MeV for the ^{16}O reaction, at a barrier radius of $R_b = 10.80$ fm with a curvature $\hbar\omega = 4.34$ MeV. The corresponding parameters for the ^{17}O reaction were $B_0 = 60.78$ MeV, $R_b = 10.86$ fm, and $\hbar\omega = 4.20$ MeV. This small difference in s -wave barrier heights is due to the change in radius required for the ^{17}O projectile. The excitation function calculated with the ^{16}O parameters is shown in Fig. 1 by the dotted line; clearly it is a poor representation of the experimental data at lower energies. By changing the parameters of the single barrier, or by introducing any other degree of

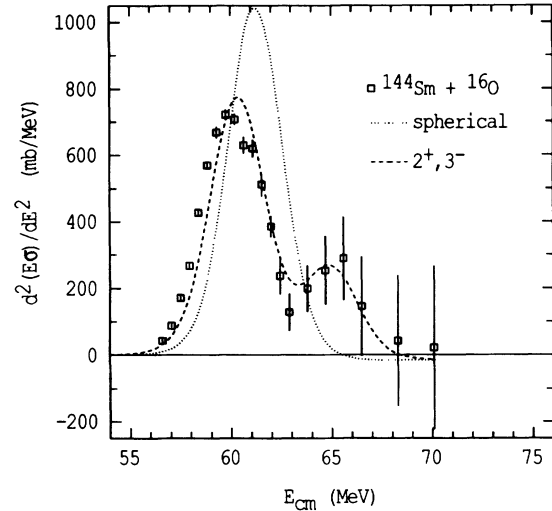


FIG. 2. The experimental fusion barrier distribution for the reaction $^{144}\text{Sm}+^{16}\text{O}$ (open squares). The dotted line is the theoretical distribution for a single barrier. The dashed line is the distribution produced with a CCMOD calculation which includes the 2^+ and 3^- states in ^{144}Sm . The theoretical barrier distributions were derived from the calculated excitation functions in the same manner as the experimental distributions.

freedom, the agreement over the full energy range can in principle be improved. It is shown below that when the data and calculations are presented in terms of the distribution of barriers, the reasons for the enhanced fusion cross sections become apparent.

The quantity $d^2(E\sigma)/dE^2$ is directly related to the distribution of barriers smoothed by barrier penetration [8]. Figure 2 shows the experimental barrier distribution for $^{144}\text{Sm}+^{16}\text{O}$ derived from the cross sections presented in Fig. 1 using the point difference formula given in Ref. [9] with an energy step of $\Delta E = 1.8$ MeV. The $d^2(E\sigma)/dE^2$ from the calculated single barrier excitation function is indicated by the dotted line in Fig. 2. The measured distribution shows that the single barrier is split into two discrete components. Previous analyses of less precise data assuming a single barrier [15] or a distribution due to a small prolate deformation [14] are inconsistent with the results presented here.

The main features of the two barrier distributions for the ^{16}O and ^{17}O induced reactions are very similar (see Fig. 3), strongly suggesting that the double-peaked distribution is due to inelastic excitations of the target. To model this, a modified version CCMOD [6] of the coupled-channels code CCDEF [16] was used. This modified program includes the excitation energies in the coupling matrix in a similar manner to CCDEF but the matrix is diagonalized at each value of the internuclear separation r . The effect of coupling to nonfusion channels is to replace the single-channel barrier with a set of barriers $B_\alpha = B_0 + \eta_\alpha$, where α represents the channel index and

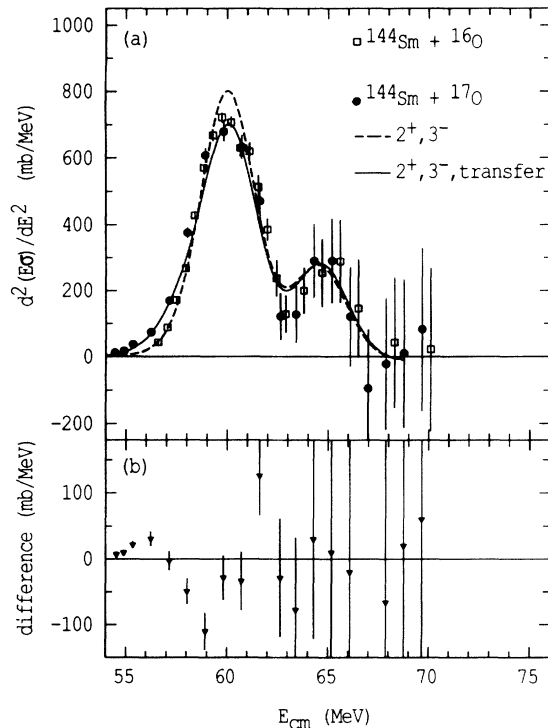


FIG. 3. (a) The experimental barrier distribution for $^{144}\text{Sm} + ^{17}\text{O}$ (solid circles) compared with the ^{16}O reaction (open squares). The solid line is a CCMOD calculation including single particle transfer with a coupling strength of 2.8 MeV. The dashed line is the same calculation without the transfer channel. (b) The difference between the $^{144}\text{Sm} + ^{17}\text{O}$ and $^{144}\text{Sm} + ^{16}\text{O}$ barrier distributions (see text).

η_α are the eigenvalues of the coupling matrix at the corresponding barrier positions. The coupling strength for inelastic excitations [16] was taken as

$$F_{\text{inel}}(r) = \frac{\beta_\lambda}{\sqrt{4\pi}} \left[-R \frac{dV_n(r)}{dr} + \frac{3Z_1 Z_2 e^2 R^\lambda}{2\lambda + 1} \frac{1}{r^{\lambda+1}} \right], \quad (1)$$

where λ is the multipolarity of the transition, β_λ is the deformation parameter of the mode, R is the radius of the nucleus which is excited, and V_n is the nuclear potential. The deformation parameter β_λ was calculated from the relevant ground-state transition strengths $B(E\lambda) \uparrow$:

$$\beta_\lambda = \frac{4\pi}{3ZR^\lambda} \left[\frac{B(E\lambda) \uparrow}{e^2} \right]^{1/2}, \quad (2)$$

with $R = 1.06A^{1/3}$ fm.

A two-channel calculation using the code CCMOD with coupling to the 3^- state of ^{144}Sm , with $B(E3) \uparrow = 0.27 e^2 \text{b}^3$ [17], was performed using the Woods-Saxon nuclear potential parameters given above. The resultant two barriers have weights and energies $(w_\alpha, B_\alpha) = (0.73, 60.42 \text{ MeV})$ and $(0.27, 64.62 \text{ MeV})$. The distribution for a three-channel calculation, with additional cou-

pling to the 2^+ state $B(E2) \uparrow = 0.266 e^2 \text{b}^2$ [18], is shown by the dashed line in Fig. 2; it is essentially the same as the two-channel calculation because of the smaller coupling strength of the 2^+ state. The agreement between experiment and the simple coupled-channels calculation is good, and confirms that coupling to single-phonon excitations of ^{144}Sm is responsible for the splitting of the distribution of barriers. Because of approximations inherent in CCMOD, the results are expected to deviate increasingly from those of an exact coupled-channels calculation as the excitation energy of the intrinsic states increases. Since the 2^+ and 3^- states in ^{144}Sm are at ≈ 2 MeV, the CCMOD calculations presented here were compared with a more exact coupled-channels calculation which demonstrated that the approximations made were reasonable in this case.

The barrier distribution for $^{144}\text{Sm} + ^{17}\text{O}$ is shown in Fig. 3(a) with the ^{16}O distribution for comparison. At the higher energies the two distributions agree within experimental uncertainty. However, the main peak of the distribution for ^{17}O is lower than that for ^{16}O . The strength missing from this peak is present at lower energies, a reflection of the threefold to fourfold increase in the cross sections for the ^{17}O reaction over ^{16}O in the energy range of $E_{c.m.} - B_0 \leq -3$ MeV (see Fig. 1). To emphasize this difference, the distribution for the ^{16}O reaction has been subtracted from that for ^{17}O , after shifting the former distribution by 0.33 MeV so that the uncoupled barriers (B_0) coincide. This difference distribution is shown in Fig. 3(b), and clearly illustrates the shift in barrier strength to lower energies. For weak coupling, barrier strength at energies below the main barrier can only be explained by coupling to a *positive* Q -value transfer reaction [19].

The code CCMOD was used to include the additional effects of transfer for the ^{17}O reaction, using the same inelastic coupling strengths as for the ^{16}O case. The transfer coupling strength \mathcal{K} was specified at the position of the unperturbed barrier, and the spatial variation of this strength [20] was taken as

$$F_{\text{tran}}(r) = \frac{\mathcal{K}}{\sqrt{4\pi}} \exp \left[-\frac{r - R_b}{1.2 \text{ fm}} \right]. \quad (3)$$

In Fig. 3(a) the solid line is the distribution produced with a CCMOD calculation by including the single neutron stripping channel with $Q = +2.6$ MeV. The dashed line is the same calculation but with no transfer channel. The inclusion of the transfer channel gives very good agreement in the low energy region. The value of \mathcal{K} which provides the best representation of the data is 2.8 MeV, compared to a previous estimate of ≈ 3 MeV [20]. Calculations have been performed assuming equal coupling to a series of single particle states in ^{145}Sm with average energies taken from Ref. [21]. An equally good representation of the data was obtained when the total coupling strength to states with $Q > 0.8$ MeV was 2.8 MeV. The

quality of the data presented here justifies the use of a full coupled-channels calculation to obtain experimental coupling strengths.

These data demonstrate again [9–11] the benefits of precise and comprehensive excitation function measurements, and show that detailed information can be extracted for this weak coupling case. Continuing to fit less precise data is unlikely to be as effective in extending our understanding of fusion.

A full understanding of near-barrier reactions requires a simultaneous analysis of inelastic scattering, transfer, and fusion excitation functions. However, it has been shown here that precisely measured fusion excitation functions convey more information than had previously been thought. In particular, by using the distribution of barriers representation, features are seen which indicate the influence of the individual channels on the internuclear potential and hence on the fusion barrier. By virtue of the choice of the fusion reactions studied here, the signatures of inelastic excitation of single phonon states and of a positive Q -value transfer reaction have been isolated and clearly identified in the fusion barrier distribution for the first time. Furthermore, quantitative information can be obtained on the strength of the coupling of fusion to inelastic and transfer channels, which can be exploited to obtain a clearer picture of the interplay of near-barrier reaction processes.

* Permanent address: SERC Daresbury Laboratory,

- Daresbury, Warrington WA4 4AD, United Kingdom.
- [1] R.A. Broglia, C.H. Dasso, and S. Landowne, *Phys. Rev. C* **32**, 1426 (1985).
 - [2] J.A. Kittl *et al.*, *Nucl. Phys.* **A471**, 587 (1987).
 - [3] E.F. Aguilera *et al.*, *Phys. Rev. C* **41**, 910 (1990).
 - [4] A. Morsad *et al.*, *Phys. Rev. C* **41**, 988 (1990).
 - [5] R.J. Tighe *et al.*, *Phys. Rev. C* **42**, 1530 (1990).
 - [6] M. Dasgupta *et al.*, *Nucl. Phys.* **A539**, 351 (1992).
 - [7] H. Funaki and E. Arai, *Nucl. Phys.* **A556**, 307 (1993).
 - [8] N. Rowley, G.R. Satchler, and P.H. Stelson, *Phys. Lett. B* **254**, 25 (1991).
 - [9] J.X. Wei *et al.*, *Phys. Rev. Lett.* **67**, 3368 (1991).
 - [10] J.R. Leigh *et al.*, *Phys. Rev. C* **47**, R437 (1993).
 - [11] R.C. Lemmon *et al.*, *Phys. Lett. B* **316**, 32 (1993).
 - [12] J.X. Wei *et al.*, *Nucl. Instrum. Methods Phys. Res., Sect. A* **306**, 557 (1991).
 - [13] J.R. Leigh *et al.*, in *Proceedings of the RIKEN International Workshop on Heavy-Ion Reactions with Neutron Rich Beams, Wako, Japan, 1993*, edited by M. Ishihara, N. Takigawa, and S. Yamaji (World Scientific, Singapore, 1993), p. 29.
 - [14] D.E. Di Gregorio *et al.*, *Phys. Rev. C* **39**, 516 (1989).
 - [15] D.E. Di Gregorio *et al.*, *Phys. Lett. B* **176**, 322 (1986).
 - [16] C.H. Dasso and S. Landowne, *Comput. Phys. Comm.* **46**, 187 (1987); J. Fernández-Niello, C.H. Dasso, and S. Landowne, *ibid.* **54**, 409 (1989).
 - [17] R.H. Spear, *At. Data Nucl. Data Tables* **42**, 55 (1989).
 - [18] S. Raman *et al.*, *At. Data Nucl. Data Tables* **36**, 1 (1987).
 - [19] C.H. Dasso, S. Landowne, and A. Winther, *Nucl. Phys.* **A407**, 221 (1983).
 - [20] R.A. Broglia *et al.*, *Phys. Lett. B* **133**, 34 (1983).
 - [21] S.T. Thornton *et al.*, *Phys. Rev. C* **12**, 877 (1975).